



OPEN Social memory deficits and their neural correlates in multiple sclerosis

André Magalhães^{1,6}, Marta Morais^{1,6}, Liliana Amorim², Ana Coelho¹, Rafaela Morais-Ribeiro¹, Celina Gomes³, Tiago Gil Oliveira^{1,4}, Matthew Schafer⁵, João Cerqueira^{1,3} & Torcato Meira^{1,4}✉

While the impact of multiple sclerosis (MS) on various cognitive functions has been well documented, social memory - memory of other individuals - remains unexplored. In this study, 26 MS patients and 23 healthy controls underwent task-based fMRI during a social navigation paradigm simulating interpersonal interactions, followed by an episodic social memory recall questionnaire. T1-weighted, T2-FLAIR and diffusion tensor imaging were also acquired. As social navigation metrics have been associated with activity in the precuneus/posterior cingulate cortex (PPCC), we examined this region's functional and volumetric correlates, as well as T2-FLAIR hyperintense white matter lesion burden and microstructural abnormalities in normal-appearing white matter. MS patients showed preserved social navigation but impaired episodic social memory ($p = 0.003$). No task-based functional differences were observed between groups. However, impaired recall in MS was associated with reduced right PPCC volume ($p = 0.032$), greater volume ($p = 0.002$) and number ($p = 0.017$) of T2-FLAIR hyperintense lesions, and altered integrity of normal-appearing white matter, indexed by lower fractional anisotropy ($p < 0.001$) and higher mean diffusivity ($p = 0.019$). These findings suggest a novel cognitive deficit in MS and underscore the potential relevance of regional brain volume and white matter pathology to social memory, informing future studies of social cognition in MS and other neuropsychiatric disorders.

Keywords Social memory, Multiple sclerosis, White matter lesion load, Normal-appearing white matter, Precuneus, Posterior cingulate cortex

Multiple sclerosis (MS) is one of the most common causes of non-traumatic disability among young adults¹. It is a chronic inflammatory, demyelinating, and neurodegenerative disease of the central nervous system, with neurodegenerative processes, which manifests, among other changes, as progressive accumulation of T2-hyperintense white matter lesions, microstructural abnormalities in normal-appearing white matter, and atrophy of multiple brain structures, detectable through magnetic resonance imaging (MRI)². Besides being classically defined by motor and sensory symptoms, MS also affects cognition in 40–70% of patients³, with cognitive impairment contributing to reduced employment, lower quality of life, and poorer adherence to treatment^{4–8}. While cognitive deficits such as those affecting processing speed, executive functions, attention, working memory, verbal episodic memory, and visuospatial episodic memory have been consistently studied in MS^{3,9}, other functions, particularly within the social cognitive domain, remain comparatively understudied. Social cognition refers to the set of cognitive functions that enable individuals to process, store, recognize, manipulate, and apply socially relevant information^{10,11}. In MS, some impairments in social cognition have been documented¹¹, including difficulties in facial emotion recognition¹² and theory of mind - the ability to infer others' thoughts, feelings, and beliefs^{12,13}. Increasing evidence has linked these deficits to both grey matter pathology^{13–16} and white matter damage^{12,13,17–20}, and studies using resting-state functional imaging have highlighted the involvement of frontal and temporal networks in these alterations^{21–24}. However, other components of social cognition, such as social memory, remain largely unexplored in this population.

Social memory is a key component of declarative memory, defined as the ability to encode and retrieve the identity and previous interactions with others^{25,26}. This capacity is essential for navigating complex social environments, sustaining interpersonal bonds, and adapting behavior based on past experience²⁷. Importantly,

¹Life and Health Sciences Research Institute (ICVS), School of Medicine, University of Minho, Campus Gualtar, Braga, Portugal. ²Association P5 Digital Medical Center (ACMP5), Braga, Portugal. ³Clinical Academic Center, Braga, Portugal. ⁴Department of Neuroradiology, Hospital de Braga, ULS Braga, Braga, Portugal. ⁵Department of Psychiatry, Columbia University, New York, NY, USA. ⁶These authors contributed equally to this work: André Magalhães and Marta Morais. ✉email: torcatomeira@med.uminho.pt

deficits in social memory could plausibly contribute to the other well-documented impairments in social cognition observed in MS.

Overcoming the prior absence of suitable tools to assess social memory^{27,28}, a social navigation task was developed to mimic real-life social interaction in a dynamic process in which participants make choices during encounters with virtual characters that reflect their evolving perception of each character²⁹. These choices are used to construct an individual “social map” structured along two dimensions, power (reflecting dominance or submission) and affiliation (reflected in sharing private information or physical touch), the two main factors that influence relationships²⁹. Derived metrics from this map have been shown to predict activity in the hippocampus and in the precuneus/posterior cingulate cortex (PPCC)^{29,30}. At the end of the task, a multiple-choice questionnaire is administered to assess recall of the characters involved in specific social events encountered during its progression, providing a behavioral measure of episodic social memory retrieval²⁹. Together, the navigation task and recall questionnaire provide complementary behavioral indices of social memory, encompassing both the dynamic mapping of social relationships and the explicit retrieval of socially relevant episodes.

In the present study, we aimed to assess social memory function in people with MS using a behavioral framework that included a social navigation task performed during task-based functional MRI acquisition, and an episodic social memory recall questionnaire. We hypothesized that MS patients would show impaired social memory. In addition, we sought to investigate whether differences in social memory performance were associated with functional or structural brain changes. Specifically, we predicted that lower social memory performance in MS would be associated with reduced volume (as measured on T1-weighted imaging) or altered activity of the hippocampus or PPCC, higher T2-hyperintense white matter lesion burden, and greater microstructural abnormalities in normal-appearing white matter as assessed by diffusion tensor imaging metrics. We report novel evidence suggesting that MS patients exhibit impairments in episodic social memory recall, which correlate with right PPCC volume and white matter lesion load.

Results

Behavioral data: social navigation and episodic social memory recall

We first characterized participants’ behavioral profiles, focusing on two distinct components of social memory: social navigation and episodic social memory recall. Demographic and clinical characteristics, including age, sex, educational level, and Hospital Anxiety and Depression Scale (HADS) scores, are presented in Table 1. For the MS group, we additionally report time since first symptom, total number of relapses, Expanded Disability Status Scale (EDSS) score, and Modified Fatigue Impact Scale (MFIS) score. No significant group differences were found in any of these variables.

To assess implicit social navigation, we analyzed the final cosine and vector length values for each character (Fig. 1), using two-way ANOVAs with group (MS vs. healthy controls) as a between-subject factor and character identity (C1–C5) as a within-subject factor. Analyses revealed a significant main effect of character identity for both metrics (Fig. 2), but no significant main effect of group (cosine: $p = 0.986$; vector length: $p = 0.726$) or group-by-character interaction (cosine: $p = 0.512$; vector length: $p = 0.536$). Multiple post-hoc pairwise differences between characters were identified. Similarly, when participants were asked to explicitly place each character on a two-dimensional affiliation–power map at the end of the task, their placements did not differ between groups (Supplementary Fig. S1).

In contrast, MS patients scored significantly lower than healthy controls on the questionnaire designed to assess episodic social memory recall - defined as the conscious retrieval of specific social interactions and events ($p = 0.003$; MS median = 25; controls median = 21) (Fig. 2). To determine whether this difference could

Variable	MS group (n = 26)	Control group (n = 23)	p value
Age [years (Q1–Q3)]	36.5 (18–54)	35 (24–54)	0.992
Sex - Female [% (n)]	46% (12)	48% (11)	1.000
Mandatory education only [% (n)]	38% (10)	26% (6)	0.382
Total HADS [score (Q1–Q3)]	11 (4–25)	10 (0–21)	0.154
Time since first symptom [years (Q1–Q3)]	11 (1–29)	-	-
Total number of relapses [n (Q1–Q3)]	2 (1–22)	-	-
EDSS [score (Q1–Q3)]	1 (0–3)	-	-
MFIS [score (Q1–Q3)]	34 (2–57)	-	-

Table 1. Demographic and clinical characteristics of the MS and control groups. Continuous variables are presented as median (Q1–Q3), and categorical variables are shown as percentages with absolute counts in parentheses. Group comparisons for continuous variables were performed using the Mann–Whitney U test, with no significant differences for age ($U = 298.5$, $Z = -0.01$, $r = -0.00$, $p = 0.992$) or total HADS score ($U = 370.0$, $Z = 1.43$, $r = 0.20$, $p = 0.154$). Comparisons of categorical variables were conducted using Fisher’s exact test, which revealed no significant differences in sex ($p = 1.000$) or educational level ($p = 0.382$). Disease-specific variables (time since first symptom, time since diagnosis, number of relapses, EDSS score, and MFIS score) are reported for the MS group only. HADS: Hospital Anxiety and Depression Scale; EDSS: Expanded Disability Status Scale; MFIS: Modified Fatigue Impact Scale.

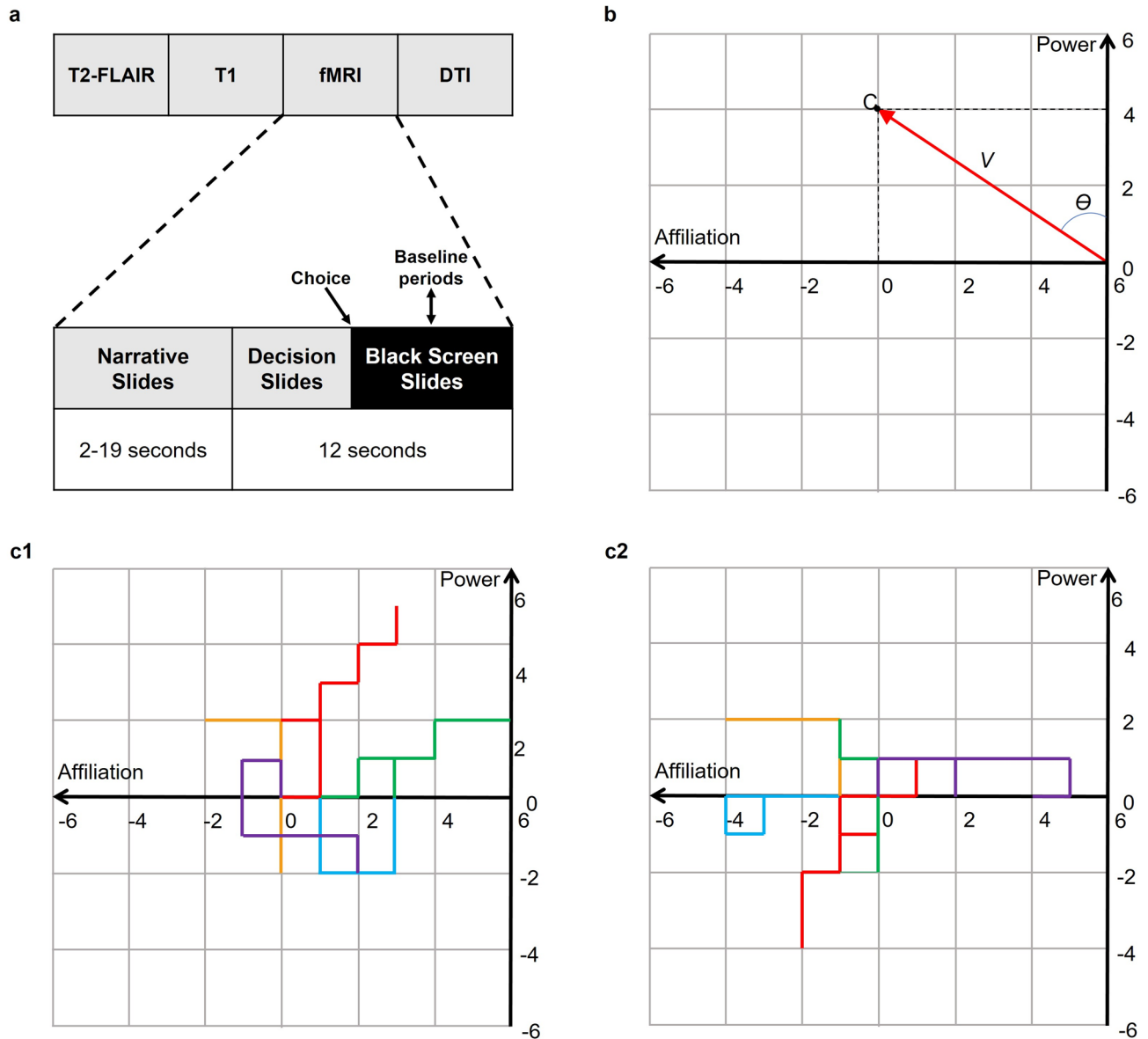


Fig. 1. Schematic representation of the social navigation task performed during fMRI. **(a)** Overview of MRI acquisition sequence and structure of the social navigation task. MRI scans were acquired in the chronological order shown from left to right: T2-weighted FLAIR imaging, T1-weighted imaging, task-based fMRI, and diffusion tensor imaging (DTI). fMRI was acquired during a structured, narrative-driven task in which participants assumed the role of a person relocating to a new city. The task included three types of slides: narrative slides, which presented contextual information or character dialogue; decision slides, in which participants chose between two response options; and black slides, which served as a “baseline” for fMRI analysis. Each decision slide was followed by a black screen upon the participant’s response; together, these lasted a total of 12 s. **(b)** Conceptual representation of the latent social space underlying the task. This two-dimensional space was defined by orthogonal axes of affiliation (x-axis; related to intimacy, empathy, or emotional closeness) and power (y-axis; related to hierarchy, dominance, or authority). Prior to the experiment, all possible interaction options were pre-classified as reflecting either affiliation or power, with each choice scored as +1 or –1 depending on whether it reinforced or opposed the respective dimension. These cumulative scores determined the evolving position of each character (C) in the social space, relative to a fixed central position representing the participant (6,0). The resulting position of each character was represented as a vector (V), with the angle (θ) encoding the relative weighting between power and affiliation in the relationship, and the length indicating the character’s distance in this latent space. **(c1, c2)** Example social maps from two participants. Each map illustrates the trial-by-trial trajectory of the five main characters through the two-dimensional power-affiliation space. Colored lines represent the cumulative path of each character, beginning at the neutral origin (0, 0) and evolving according to the participant’s decisions across 12 interactions. The maps demonstrate individual variability in how social relationships were shaped throughout the task.

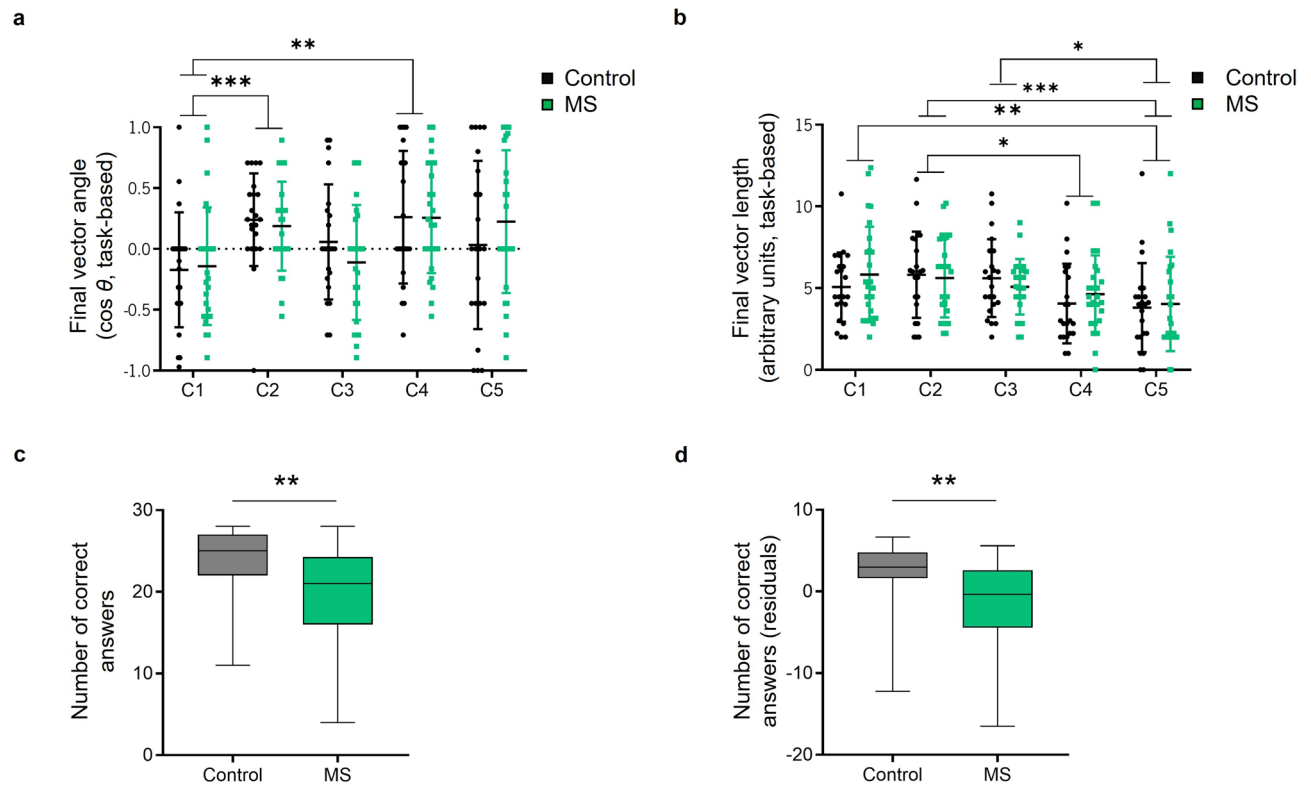


Fig. 2. Group comparison of social navigation metrics and episodic social memory recall. **(a)** Cosine of the final vector angle associated with each of the 5 main characters (C1–C5), reflecting the direction of the social vector in the power-affiliation space at task end. A two-way ANOVA revealed a significant main effect of character identity ($F(3.46, 159) = 5.71, \eta^2_p = 0.11, p < 0.001$), while the effect of group ($F(1, 46) = 0.00, \eta^2_p = 0.00, p = 0.986$) and the interaction term ($F(4, 184) = 0.82, \eta^2_p = 0.12, p = 0.512$) were not significant. Post-hoc Tukey's multiple comparisons test showed significant differences between C1 and C2 ($p < 0.001$) and C1 and C4 ($p = 0.004$), while other comparisons were not significant. **(b)** Final vector length, representing social distance, for each character. A two-way ANOVA again revealed a significant main effect of character ($F(3.82, 176) = 6.60, \eta^2_p = 0.13, p < 0.001$), with no significant effect of group ($F(1, 46) = 0.12, \eta^2_p = 0.00, p = 0.726$) or interaction ($F(4, 184) = 0.79, \eta^2_p = 0.02, p = 0.536$). Post-hoc Tukey's multiple comparisons test revealed shorter distances for character C5 relative to C1 ($p = 0.009$), C2 ($p < 0.001$), and C3 ($p = 0.018$), as well as a difference between C2 and C4 ($p = 0.019$). All other comparisons were not significant. **(c)** Performance on the episodic social memory recall questionnaire, in which participants were asked to identify which of the 6 characters was involved in specific social events of the storyline. MS patients correctly identified fewer characters than healthy controls, reflecting lower memory performance ($U = 154, Z = -2.93, r = -0.42, p = 0.003$, Mann–Whitney test). **(d)** Residual memory scores derived from a linear regression model in which age, sex, educational level, and HADS score were included as predictors of the number of correct responses on the episodic social memory questionnaire. The residuals, representing the portion of variance not explained by these covariates, were then compared between groups. A significant difference between groups remained ($U = 168, Z = -2.62, r = -0.37, p = 0.009$, Mann–Whitney test). Panels a and b show group means and standard deviations, with individual data points overlaid. Panels c and d display boxplots representing medians and interquartile ranges. C1–C5 correspond to the five main characters in the storyline, labeled according to the order in which they were introduced. MS: $n = 26$; Controls: $n = 22$. $p^* < 0.05$; $** p < 0.01$; $*** p < 0.001$.

be explained by demographic variables or symptoms of anxiety and depression, we used a linear regression model to predict questionnaire scores based on age, sex, educational level, and HADS scores. We then compared the residuals - representing performance unexplained by these variables - between groups. The difference in performance remained significant after this adjustment ($p = 0.009$) (Fig. 2). Furthermore, exploratory analyses revealed that worse episodic social memory recall was associated with longer disease duration (time since first symptom), greater number of relapses, and higher EDSS scores within the MS group, while no significant correlation was found with MFIS score (Supplementary Fig. S2). No significant group differences were found in any of the additional cognitive or self-report questionnaires, including global cognition (Montreal Cognitive Assessment - MoCA), social anxiety and avoidance (Liebowitz Social Anxiety Scale), general self-efficacy (General Self-Efficacy Scale), personality traits (Neuroticism, Conscientiousness from the NEO Five-Factor Inventory), or subjective social status across three domains (MacArthur Scale for society, neighborhood, and employment) (Supplementary Fig. S1).

Neuroimaging correlates of social memory dysfunction

Given the behavioral evidence for deficits in social memory, we next investigated whether neural correlates in the hippocampus and PPCC - regions implicated in social navigation^{29,30} - might underlie this impairment. Prior studies had shown that the cosine of the social vector angle correlates with hippocampal activity, while vector length correlates with activity in the PPCC.

Group comparisons of blood oxygenation level dependent (BOLD) signal revealed no significant differences, using both region-of-interest (ROI)-based analyses (with cosine angle as predictor for hippocampal BOLD and vector length for PPCC BOLD) or whole-brain approaches. Similarly, within-group analyses did not identify significant associations in these regions or elsewhere. In these analyses, no clusters emerging at uncorrected thresholds ($p < 0.001$) survived correction for multiple comparisons using family-wise error (FWE).

Structurally, MS patients showed significantly reduced hippocampal volumes bilaterally compared to healthy controls (Fig. 3). While smaller hippocampal volumes in MS patients tended to be associated with worse episodic social memory recall, these correlations were not statistically significant (Fig. 3). No group differences were observed in PPCC volume (Fig. 3); however, within the MS group, smaller right-sided PPCC volumes were significantly associated with lower episodic social memory recall scores ($p = 0.032$), with a similar but non-significant trend on the left ($p = 0.063$) (Fig. 3). These associations remained directionally consistent, although not statistically significant, when volumetric measures were correlated with residual memory scores derived from a model controlling for age, sex, education, and HADS scores (Supplementary Fig. S3).

Given the central role of white matter pathology in MS - manifesting both as visible lesions and more diffuse microstructural abnormalities - we investigated whether white matter integrity was associated with episodic social memory recall. Lesion burden was first quantified using a segmentation tool for T2-hyperintense white matter lesions visible on T2-FLAIR images, yielding estimates of total lesion count and lesion volume. As expected, MS patients exhibited significantly higher lesion counts and lesion volume compared to healthy controls (Fig. 4). Importantly, in the MS group, higher lesion count ($p = 0.017$) and greater lesion volume ($p = 0.002$) were both significantly associated with poorer performance on the episodic social memory recall questionnaire (Fig. 4). After adjusting for age, sex, educational level, and HADS score, the association with lesion volume remained statistically significant ($p = 0.002$) (Supplementary Fig. S4).

To assess the contribution of microstructural damage in normal-appearing white matter, we analyzed diffusion tensor imaging metrics. As expected, MS patients showed reduced fractional anisotropy and increased mean diffusivity in white matter regions without T2-FLAIR hyperintensity compared to healthy controls (Fig. 5). In the MS group, both lower fractional anisotropy ($p < 0.001$) and higher mean diffusivity ($p = 0.019$) (Fig. 5) in normal-appearing white matter were significantly associated with worse performance on the episodic social memory recall task. These associations remained statistically significant after adjusting for age, sex, educational level, and HADS score (fractional anisotropy: $p = 0.007$; mean diffusivity: $p = 0.009$) (Supplementary Fig. S5).

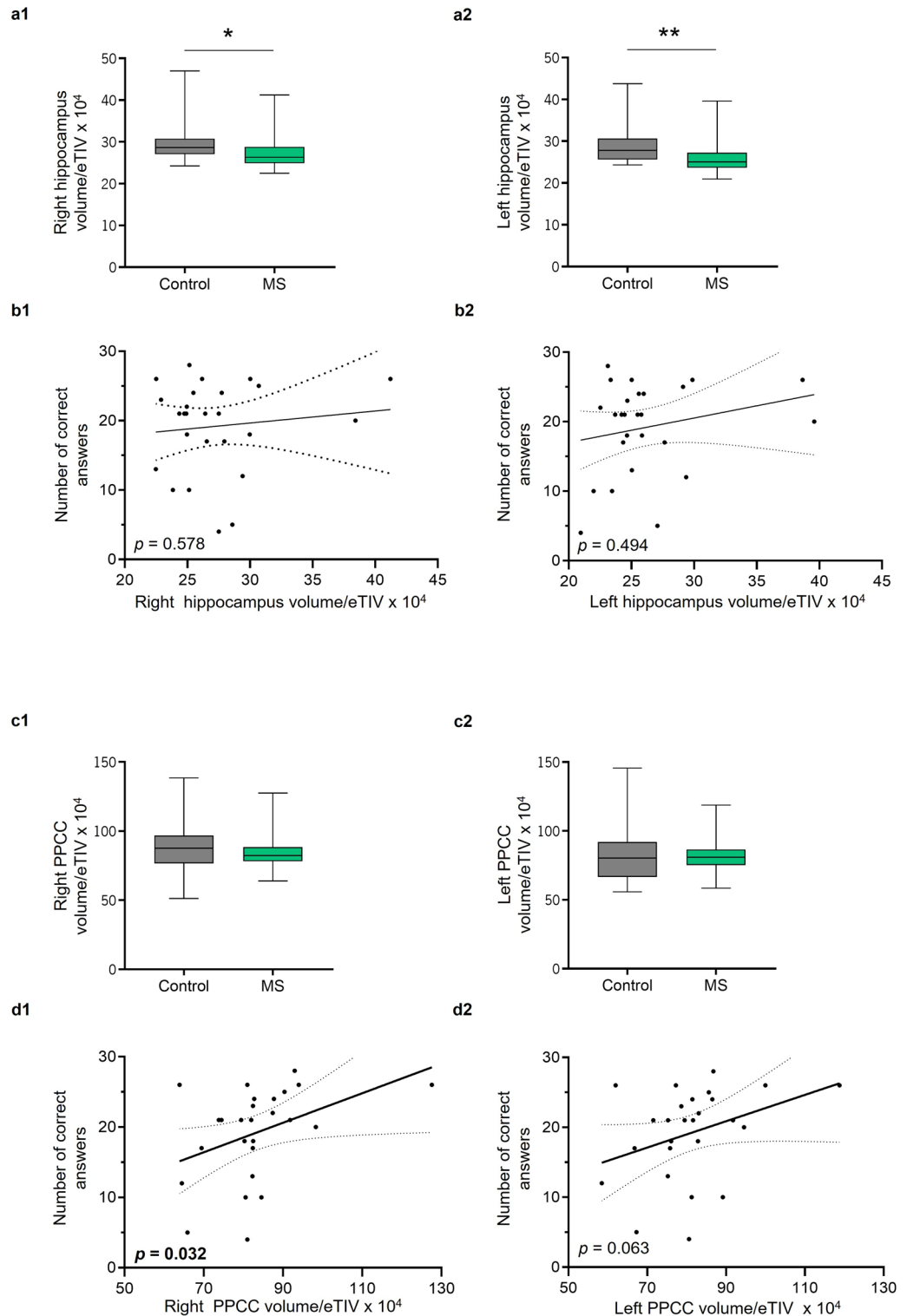
Discussion

In addition to motor and sensory symptoms, cognitive impairment is highly prevalent in MS, affecting approximately 40–70% of patients³ and contributing to higher rates of unemployment, poorer quality of life, and reduced treatment adherence^{4–8}. Nonetheless, certain cognitive functions - including social memory - remain understudied, often due to the lack of reliable assessment tools^{27,28}. In this context, our study provides novel evidence of a deficit in episodic social memory in MS, along with insights into its neural correlates.

Our findings are consistent with previous reports of declarative episodic memory impairment in MS, particularly in verbal and visuospatial domains^{3,9}, and it remains unclear whether social memory deficits reflect a distinct phenomenon or part of broader episodic memory dysfunction. Importantly, in our study, while recall of social episodes was significantly impaired in the MS group, social navigation performance was comparable between groups, suggesting the retrieval of discrete social experiences and the construction of broader “social space” representations may rely on at least partially distinct cognitive and neural mechanisms. Although our social memory questionnaire assessed recall performance, the observed deficit may reflect impairments during encoding, retrieval, or both; future work should explicitly disentangle these processes, similar to what has been done in animal models³¹ and in studies of verbal episodic memory in MS³². Social memory deficits in MS may also reflect the influence of other impaired domains, consistent with network-based analyses in healthy individuals showing that various cognitive functions, including social cognition, executive function, working memory, and language, are interrelated, forming components of a cognitive network³³.

These findings also expand the understanding of social cognitive deficits in MS, adding to the established literature on theory of mind¹¹. Notably, while theory of mind deficits are not consistently associated with disease duration or disability¹³, we found that episodic social memory recall performance was significantly associated with disease duration, number of relapses, and EDSS scores, suggesting that it may reflect cumulative disease burden. Moreover, the presence of these deficits in patients with otherwise preserved global cognition mirrors previous findings showing a dissociation between theory of mind and general cognitive performance¹³, positioning episodic social memory recall as a potentially sensitive marker of disease progression.

Although previous studies using this task have reported associations between social navigation metrics and activity in the hippocampus and PPCC in healthy individuals^{29,30}, we did not replicate those findings in our control group. This divergence may reflect technical and sample-related differences. While earlier studies employed relatively homogeneous samples, our participants were recruited from a more naturalistic, community-based population, with broader variability in age and educational level (Table 1), in a different linguistic and cultural background. In particular, variations in how participants interpret social cues or assign meaning to the narrative may have influenced neural responses to the task. Furthermore, the naturalistic structure of the task, while enhancing ecological validity, introduces behavioral variability that may obscure subtle neural effects in smaller



samples. Additionally, although the cosine and vector length metrics were used based on prior studies, they may not fully capture the complexity of social mapping mechanisms. Importantly, the task nonetheless demonstrated behavioral sensitivity in the differentiation between characters observed across both groups. Whether preserved social navigation in MS is maintained through undetected compensatory neural mechanism remains unclear and could be further explored using complementary approaches, such as with resting-state fMRI.

Whereas functional activation of the hippocampus and PPCC did not differ between groups, we observed bilateral hippocampal atrophy in MS patients, consistent with previous reports³⁴, along with a significant association between reduced right PPCC volume and poorer recall performance. Our volumetric data suggest that the PPCC - and possibly the hippocampus - may contribute to episodic social memory retrieval. This interpretation is supported by prior evidence implicating the posterior cingulate cortex³⁵ and the precuneus^{35,36} in other episodic memories retrieval. In addition, reduced precuneus volume has been associated with impaired

Fig. 3. Volume of the hippocampus and PPCC - comparison between groups and association with episodic social memory recall in MS. **(a1, a2)** Comparison of hippocampal volume adjusted to eTIV between MS and control participants. MS patients exhibited significantly reduced right hippocampal volume (a1; $U=187$, $Z=-2.24$, $r=-0.32$, $p=0.025$, Mann–Whitney test) and left hippocampal volume (a2; $U=156$, $Z=-2.87$, $r=-0.41$, $p=0.004$, Mann–Whitney test). **(b1, b2)** Association between hippocampal volume/eTIV and performance on the episodic social memory questionnaire in the MS group. Both right (b1; $\rho=0.11$, $p=0.578$, Spearman correlation) and left (b2; $\rho=0.14$, $p=0.494$, Spearman correlation) hippocampal volumes showed a non-significant trend toward lower volume being associated with fewer correct responses. **(c1, c2)** No significant group differences were found in PPCC volume/eTIV, either in the right (c1; $U=256$, $Z=-0.86$, $r=-0.12$, $p=0.389$, Mann–Whitney test) or left hemisphere (c2; $U=276$, $Z=-0.46$, $r=-0.07$, $p=0.645$, Mann–Whitney test). **(d1, d2)** In the MS group, right PPCC volume/eTIV was significantly and positively correlated with the number of correct responses on the episodic social memory questionnaire (d1; $\rho=0.42$, $p=0.032$, Spearman correlation). A similar, non-significant trend was observed for the left PPCC (d2; $\rho=0.37$, $p=0.063$, Spearman correlation). Boxplots display medians and interquartile ranges; scatterplots represent individual MS patients. Regression lines and 95% confidence intervals are shown for panels b1, b2, d1, and d2. P -values from each Spearman correlation are displayed in the bottom-left corner of each scatterplot; significant values ($p < 0.05$) appear in bold. MS: $n=26$; Controls: $n=23$. * $p < 0.05$; ** $p < 0.01$; eTIV, estimated total intracranial volume.

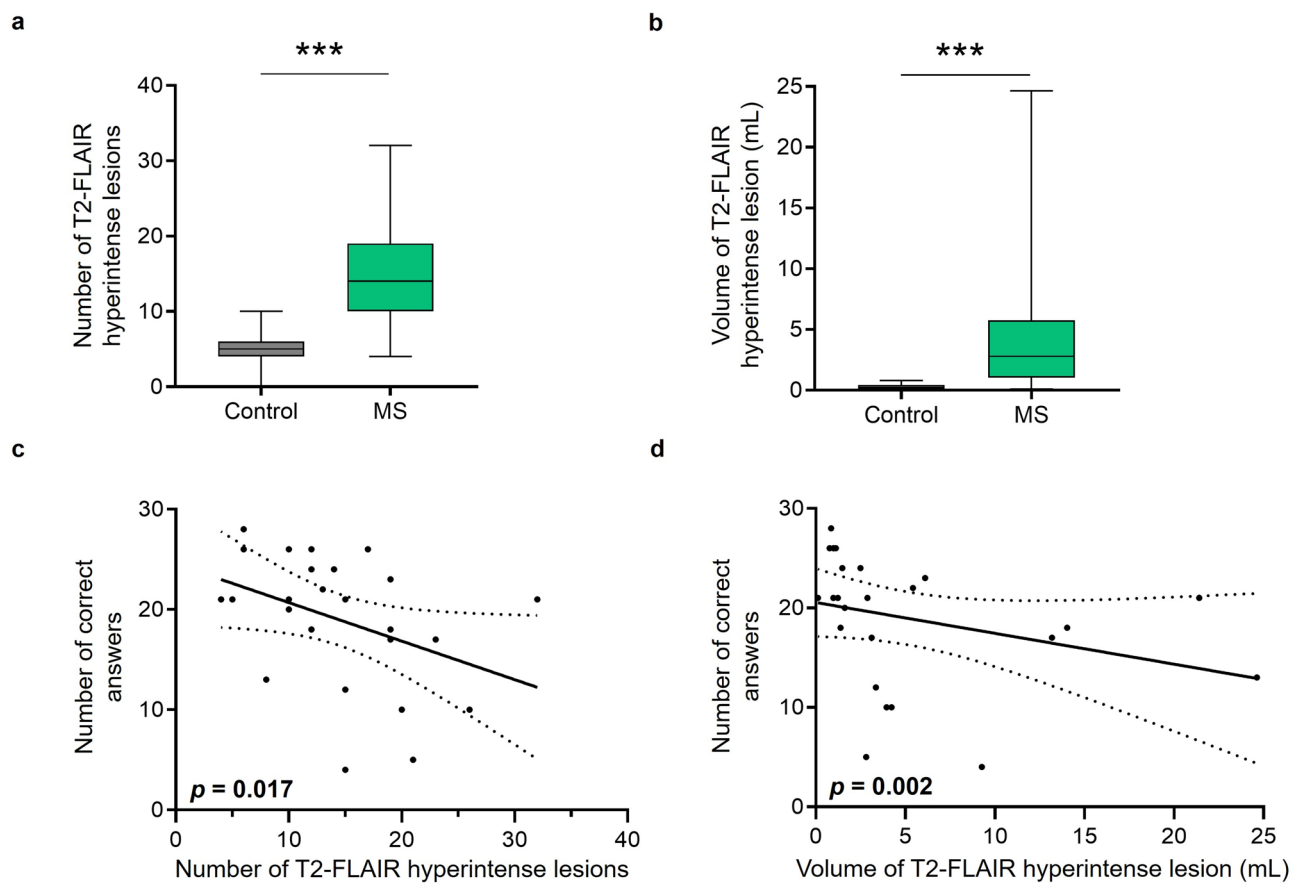


Fig. 4. T2-FLAIR hyperintense white matter lesion load and its association with episodic social memory recall in MS. **(a)** Total number of T2-FLAIR hyperintense white matter lesions. MS patients exhibited significantly higher lesion counts than healthy controls ($U=537$, $Z=5.17$, $r=0.75$, $p < 0.001$, Mann–Whitney test). **(b)** Total volume of T2-FLAIR hyperintense white matter lesions. Lesion volume was significantly greater in the MS group ($U=557$, $Z=5.56$, $r=0.80$, $p < 0.001$, Mann–Whitney test). **(c)** Association between total lesion count and the number of correct responses on the episodic social memory questionnaire in the MS group. A significant negative correlation was observed ($\rho = -0.47$, $p = 0.017$, Spearman correlation), indicating that higher lesion count was associated with poorer memory performance. **(d)** Lesion volume was also significantly and negatively correlated with the number of correct responses on the episodic social memory questionnaire ($\rho = -0.60$, $p = 0.002$, Spearman correlation). Boxplots display medians and interquartile ranges; scatterplots represent individual MS patients. Regression lines and 95% confidence intervals are shown in panels c and d. P -values from each Spearman correlation are displayed in the bottom-left corner of each scatterplot. MS: $n=25$; Controls: $n=23$. *** $p < 0.001$.

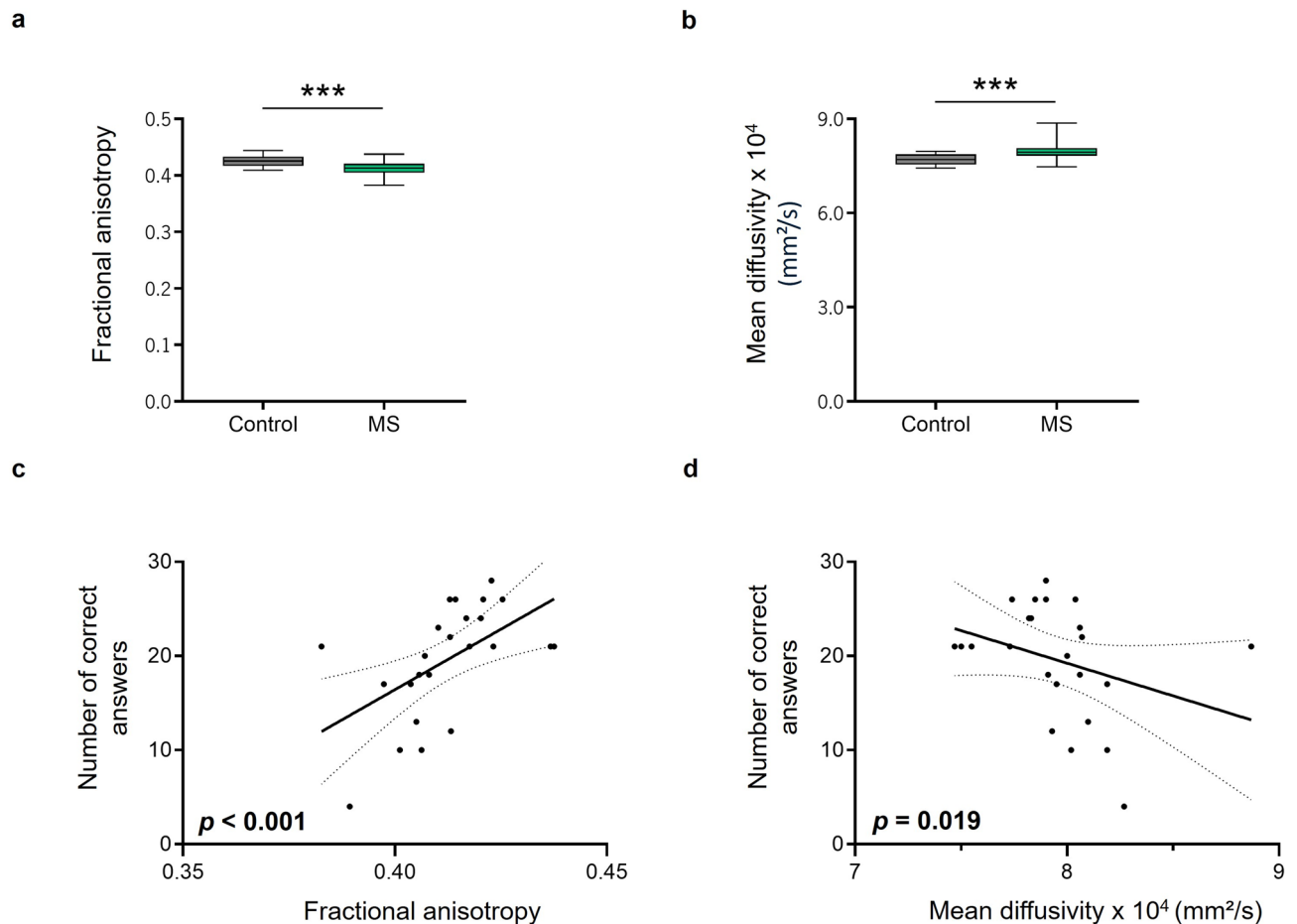


Fig. 5. Normal-appearing white matter diffusion metrics and their association with episodic social memory recall in MS. **(a)** Fractional anisotropy in normal-appearing white matter. MS patients exhibited significantly lower FA compared to healthy controls ($U = 109$, $Z = -3.41$, $r = -0.50$, $p < 0.001$, Mann–Whitney test). **(b)** Mean diffusivity in normal-appearing white matter. Mean diffusivity was significantly higher in the MS group ($U = 421$, $Z = 3.45$, $r = 0.51$, $p < 0.001$, Mann–Whitney test). **(c)** Association between fractional anisotropy and performance on the episodic social memory questionnaire in the MS group. A significant positive correlation was observed ($\rho = 0.65$, $p < 0.001$, Spearman correlation), indicating that lower fractional anisotropy was associated with poorer memory performance. **(d)** Mean diffusivity was significantly and negatively correlated with the number of correct responses on the episodic social memory questionnaire ($\rho = -0.48$, $p = 0.019$, Spearman correlation), indicating that higher MD was associated with worse memory performance. Boxplots display medians and interquartile ranges; scatterplots represent individual MS patients. Regression lines and 95% confidence intervals are shown in panels c and d. *P*-values from each Spearman correlation are displayed in the bottom-left corner of each scatterplot. MS: $n = 24$; Controls: $n = 22$. *** $p < 0.001$.

social cognition³⁷, while posterior cingulate gyrus volume has been specifically linked to theory of mind performance^{13,38}. Likewise, hippocampal atrophy has been related to deficits in verbal^{34,39} and visuospatial episodic memory³⁹. While MS is classically characterized by demyelinating white matter lesions, it is also increasingly recognized as a condition of widespread neurodegeneration and grey matter pathology, including parenchymal atrophy^{40–43}, potentially reflecting both neuronal^{44,45} and synaptic loss⁴⁵. Importantly, grey matter damage has consistently shown stronger associations with cognitive impairment than white matter abnormalities^{46,47}. Our results therefore contribute to the growing literature implicating cortical atrophy in cognitive decline in MS^{48,49}. Given the heterogeneity of the hippocampus along its longitudinal axis in terms of gene expression, electrophysiology, connectivity, and function^{50,51}, future studies could explore whether subregional volumetric differences, particularly along the anterior-posterior axis⁵², might serve as more sensitive markers of social memory dysfunction in MS. Moreover, reductions in the volume of subcortical grey matter structures, including the thalamus^{53,54} and basal ganglia⁵⁴, have also been associated with cognitive impairment in MS and warrant investigation in the context of social memory. Finally, while our findings rely solely on cross-sectional structural data, longitudinal changes in regional brain volume may provide complementary insight into cognitive dysfunction in MS⁵⁵.

Our findings also underscore the relevance of white matter pathology in episodic social memory dysfunction. Although traditionally underappreciated, white matter integrity is now increasingly recognized as fundamental

to cognition⁵⁶, and more specifically to social cognition⁵⁷. In MS, both T2-FLAIR hyperintense lesions and microstructural abnormalities in normal-appearing white matter represent hallmarks of its pathology and contribute to cognitive dysfunction³. In particular, T2-hyperintense lesions have been linked to deficits in theory of mind and facial emotion recognition¹². In the present study, both greater lesion volume and higher lesion count were associated with poorer episodic social memory recall. However, only the association with lesion volume remained statistically significant after adjusting for age, sex, education, and symptoms of anxiety and depression. This supports the notion that lesion volume may more accurately reflect the functional impact of white matter damage on distributed cognitive networks than lesion count, which may be underestimated due to lesion confluence. These findings are consistent with prior studies linking lesion volume to cognitive impairment^{58,59}. Interestingly, there is considerable histopathological heterogeneity in demyelination, and it remains unclear whether distinct patterns of demyelination⁶⁰, axonal injury⁶¹, remyelination⁶², or the presence of chronic active lesions⁶³ differentially impact social memory function. Beyond T2-FLAIR hyperintense lesions, normal-appearing white matter exhibits diffuse damage, including widespread inflammation, microglial activation, and axonal loss⁶⁴. In line with this, MS patients in our study exhibited significantly reduced fractional anisotropy and increased mean diffusivity in normal-appearing white matter, reflecting diffuse microstructural damage. Crucially, both lower fractional anisotropy and higher mean diffusivity were significantly associated with poorer episodic social memory recall performance, and these associations remained robust after adjusting for age, sex, education, and symptoms of anxiety and depression. These findings align with prior studies reporting associations between fractional anisotropy and mean diffusivity metrics of white matter and verbal or visuospatial episodic memory performance in MS⁶⁵. Reductions in fractional anisotropy particularly in normal-appearing white matter have also been associated with cognitive impairment⁶⁶. Furthermore, reduced fractional anisotropy and increased mean diffusivity across widespread white matter tracts have been associated with social cognitive deficits in theory of mind in MS¹⁸. Although our analysis focused on global diffusion metrics, future studies with larger samples employing tract-specific approaches could provide more precise insights into disconnection mechanisms underlying social memory deficits in MS.

While our findings indicate macroscale neural correlates of social memory impairment in MS, the specific circuits involved remain undefined. In rodent models, social memory has been shown to depend on the activity of distinct hippocampal subregions, particularly dorsal CA2 and ventral CA1, as well as projections from the latter to the nucleus accumbens^{31,67}. Future studies could specifically investigate whether alterations in these hippocampal subfields or their downstream projections contribute to episodic social memory deficits in MS. Hippocampal CA2 subregion, in particular, displays a distinctive molecular profile⁶⁸, including high expression of vasopressin receptor 1b and oxytocin receptor, positioning it as a potential hub for neuromodulatory regulation of social memory^{69,70}. Moreover, the unique molecular signature of CA2 also makes it an appealing therapeutic target - for instance, through pharmacological modulation of TREK-1 channels using agents such as selective serotonin reuptake inhibitors^{71,72}.

This was a unicentric, observational, and cross-sectional study, which limits the extent to which causal inferences can be made. The relatively small sample size reduces statistical power and limits the generalizability of our findings. Moreover, the inclusion of only mildly impaired patients (EDSS < 4) was necessary to ensure the feasibility of the task but restricts extrapolation to individuals with more advanced disease. Additionally, the social memory deficit we report may be influenced by other cognitive domains that are frequently affected in MS, as discussed above. Although the MoCA did not reveal significant group differences, this may reflect the limited scope and sensitivity of the screening tool. Future studies with larger samples and more comprehensive cognitive assessment will be needed to better disentangle the contribution of other cognitive processes to social memory impairment. Finally, although the task captures relevant aspects of social interaction, it does not fully reflect the complexity and personal specificity of real-world social experiences. More immersive or individually tailored paradigms may be better suited to detect subtler deficits.

In conclusion, this study provides seminal evidence of a novel cognitive deficit in MS - impaired episodic social memory - and identifies associated structural correlates involving both grey and white matter. While these findings should be interpreted with caution given the study's limitations, they contribute to refining the cognitive characterization of MS. This approach may also be extended to other neuropsychiatric conditions in which social memory may be affected.

Methods

Participants and study design

MS patients were recruited from Neurology outpatient consultations at Hospital de Braga, Portugal. Inclusion criteria were: age between 18 and 55 years, and a diagnosis of relapsing-remitting or secondary progressive MS according to the 2017 McDonald criteria⁷³. Exclusion criteria were: EDSS score ≥ 4 (used to exclude individuals with relevant physical disability that could compromise task execution or introduce confounding variability in cognitive performance); corticosteroid use within 8 weeks prior to cognitive and neuroimaging assessment; a history of other neurodegenerative or systemic diseases affecting the central nervous system; history of head trauma with loss of consciousness; a history of substance use disorders; current use of medications with potential cognitive effects (trospium chloride, oxybutynin, tricyclic antidepressants, amphetamines, or modafinil); illiteracy or inability to understand written informed consent; and any contraindication to MRI. Control participants were recruited via patient referral, typically acquaintances or family members, and were required to meet the same inclusion and exclusion criteria, except those specifically related to MS. Demographic and clinical data collected included age, sex, educational level (dichotomized as up to mandatory schooling - i.e., completion of 12 years of formal education - versus higher education), HADS score, and MFIS score. For the MS group, additional variables were recorded: time since first symptom, number of relapses, and EDSS score. All participants were subsequently contacted to schedule the behavioral and neuroimaging assessment session.

Importantly, all participants who met inclusion criteria and were recruited successfully completed the cognitive and neuroimaging assessments. No exclusions occurred between recruitment and evaluation. Missing data in some analyses were solely due to technical issues during MRI acquisition or task execution, as detailed below. The session began with MRI acquisition and completion of the social navigation task, followed by the episodic social memory recall questionnaire, explicit spatial mapping of social relationships, global cognitive testing, and psychosocial self-report measures (described below). All participants provided written informed consent prior to participation. The study was approved by the Ethics Committee of Hospital de Braga (reference 173_2022). All procedures were conducted in accordance with relevant guidelines and regulations, and the research was performed in accordance with the Declaration of Helsinki. A total of 49 individuals participated in the study, including 26 MS patients and 23 healthy controls. Due to a hardware malfunction during the social navigation task, response data and corresponding fMRI measures were unavailable for one control participant, resulting in a final sample of 22 healthy controls for those analyses. Additionally, for one MS patient, the 3D T2-FLAIR sequence was not acquired due to a protocol error; consequently, T2-hyperintense lesion burden metrics were computed for 25 MS patients. Regarding diffusion imaging, data were excluded for two MS patients - one due to the missing 3D T2-FLAIR sequence and another due to incomplete acquisition - as well as for one control participant due to severe image artifacts; the final diffusion analysis thus included 24 MS patients and 22 healthy controls.

Social navigation task

The first behavioral assessment consisted of the social navigation task performed during fMRI acquisition. The task was adapted from the original paradigm described by Tavares et al.²⁹. Although not a game in the strict sense, the task followed a role-playing format: participants assumed the protagonist role of a person relocating to a new town, aiming to secure employment and housing through interactions with local residents. The task was implemented using PsychoPy 3.0 (<https://www.psychopy.org>), which controlled stimulus presentation and response collection during scanning. The total task duration was 32 min and 51 s (during which 1350 functional volumes were acquired).

Participants were presented with slides showing cartoon characters “speaking” through word bubbles. These included only character images and written text, with no spatial or contextual visual cues. Each character had distinct traits that implicitly conveyed aspects of their social role. While lying in the scanner, participants used response boxes to choose one of two predefined replies to each interactive slide. These choices were designed to shape the evolving relationship with each character and were preclassified as modulating either the power dimension (i.e., giving or receiving instructions, orders, or demands) or the affiliation dimension (i.e., engaging in personal conversation or accepting/initiating physical contact). Although the task structure resembled a “choose-your-own-adventure” narrative in terms of participant engagement, the storyline and sequence of interactions were fixed and not contingent on previous choices. Participants were instructed to respond naturally and intuitively, as they would in real-life social situations.

Each of the 5 main characters appeared in 12 interactive trials (6 affecting power, 6 affecting affiliation), and these interactions cumulatively determined the character’s trajectory within an abstract, participant-centered two-dimensional social space defined by power (vertical axis) and affiliation (horizontal axis) (Fig. 1). A sixth, neutral character was also included and appeared in 3 socially neutral interactions that did not involve shifts in power or affiliation. This character remained fixed at the center of the social space (coordinates 0,0) and served to simulate neutral social interactions, as in previous implementations of the task. At the beginning of the task, all main characters were assigned the same neutral starting position on both axes, at coordinates (0, 0). The participant’s reference point was fixed at coordinates (6, 0). The evolving relationship between participant and character was represented as a vector originating from the participant’s fixed position and pointing toward the character’s current location. With each new decision, the character moved one unit along one of the axes (up/down for power; toward/away for affiliation). These updates yielded a dynamic vector whose angle cosine represented the orientation in power-affiliation space, and whose length quantified the absolute social distance.

These parameters were computed continuously and later used to model neural activity across trials. The final position of each character reflected the cumulative outcome of interactions and served as a behavioral signature of that character’s location in the participant’s implicit social map (Fig. 1).

The task was translated into Portuguese by two independent researchers. To assess clarity and alignment with the original classifications, 10 volunteers independently labeled each of the 60 interactive trials as targeting either power or affiliation. Overall agreement with the predefined categories was approximately 98%, with 590 out of 600 classifications matching the original. Specifically, two participants disagreed on three trials each, and another two on two trials each, with discrepancies distributed heterogeneously across items. Volunteers also rated the polarity of each response (+1 or -1) based on whether the option was expected to increase or decrease power/affiliation, achieving 100% agreement with the predefined scoring system. This preliminary testing also served to estimate adequate reading times: narrative slides were displayed for 2 to 19 s, while decision slides were shown for up to 12 s (Fig. 1). Once a participant responded, the decision slide was replaced by a blank black screen, which remained visible until the 12-second window had elapsed. This allowed for a variable inter-trial interval that served as “baseline” for fMRI analysis.

Eight task versions were created to accommodate participant age and linguistic adaptations to match the participant’s gender. Four versions used older-looking characters for participants aged 35 and above, while four others used younger-looking characters. These versions also ensured balanced character gender representation.

Episodic social memory questionnaire

Immediately after the task, participants completed a 30-item multiple-choice questionnaire assessing episodic social memory recall. As no explicit instruction to memorize was given, encoding was assumed to occur implicitly

during the social navigation interactions. Each item referred to a specific social event that had occurred during the narrative (e.g., “Who invited you to dinner?”), and participants were asked to identify which character had been involved. All 6 characters from the task were included as response options for each question. Each item had a single correct answer. The questionnaire version was matched to the specific storyline used for each participant to ensure consistency in character roles and response accuracy across adapted versions. The total number of correct responses was used as a behavioral index of episodic social memory recall.

Explicit spatial evaluation of social relationships, global cognition, and psychosocial self-report measures

Participants subsequently completed an explicit spatial evaluation of social relationships, as well as global cognitive and psychosocial questionnaires. They were asked to position each of the 6 characters on a two-dimensional grid defined by power and affiliation axes, based on how they perceived each character in relation to themselves. For each character, the cosine of the social vector angle and the vector length were computed and used as metrics of participants' explicit spatial representation of social relationships. Global cognitive functioning was assessed with the MoCA. The remaining instruments were self-report measures: the Neuroticism and Conscientiousness subscales of the NEO Five-Factor Inventory were used to assess personality traits; the Liebowitz Social Anxiety Scale measured social fear and avoidance; the General Self-Efficacy Scale assessed perceived general self-efficacy; and the MacArthur Scale of Subjective Social Status evaluated subjective social rank across society, neighborhood, and employment domains.

MRI data acquisition

All scans were acquired on a 3 T Siemens Magnetom Avanto scanner using a 32-channel head coil. The protocol began with the acquisition of structural images: a 3D T2-weighted FLAIR sequence (repetition time/echo time [TR/TE] = 5000/392 ms; inversion time [TI] = 1600 ms; voxel size = 0.56 mm isotropic; 288 sagittal slices; field of view [FOV] = 250 × 250 × 161 mm), followed by a 3D T1-weighted magnetization-prepared rapid acquisition with gradient echo sequence (TR/TE = 2450/4.13 ms; TI = 1100 ms; flip angle = 9°; voxel size = 1 mm isotropic; 176 sagittal slices; FOV = 256 × 256 × 256 mm). Functional data were collected during performance of the social navigation task using a T2*-weighted echo-planar imaging sequence (TR/TE = 1460/12 ms; flip angle = 90°; voxel size = 3 mm isotropic; 44 interleaved transverse slices; anterior-to-posterior encoding; FOV 200 × 200 mm). A gradient field map with matching geometry was also acquired (TR = 700 ms; TE1/TE2 = 5.19/7.65 ms; flip angle = 54°; voxel size = 3 mm isotropic; 44 interleaved transverse slices; right-to-left encoding; FOV = 200 × 200 mm). The first 8 s of each BOLD acquisition were discarded prior to preprocessing to allow for MR signal stabilization. Diffusion-weighted data were acquired using a single-shot spin-echo echo-planar imaging sequence (TR/TE = 5600/93 ms; voxel size = 2.0 × 2.0 × 3.5 mm; 44 interleaved transverse slices; anterior-to-posterior encoding; FOV = 220 × 220 mm), with 64 non-collinear diffusion directions and b-values of 0 and 1000 s/mm². To facilitate correction of susceptibility-induced distortions, an additional image with reversed phase-encoding direction (posterior-to-anterior) was acquired using identical parameters.

MRI preprocessing and analysis

DICOM files were converted to Nifti format using `dcm2nii`⁷⁴. Structural and functional MRI preprocessing was performed using `fMRIPrep` 22.1.0⁷⁵.

T1-weighted images underwent intensity non-uniformity correction, skull stripping, tissue segmentation, cortical surface reconstruction, and normalization to Montreal Neurological Institute space. Regional brain volumes were then extracted using `FreeSurfer` utilities⁷⁶. For volumetric analysis, bilateral hippocampal and PPCC volumes were normalized to estimated total intracranial volume (eTIV) by computing the volume-to-eTIV ratio.

T2-hyperintense white matter lesion segmentation was conducted using the Lesion Prediction Algorithm from the Lesion Segmentation Toolbox v3.0.0⁷⁷ in Statistical Parametric Mapping (SPM) software⁷⁸. The algorithm was applied to 3D T2-FLAIR images to generate lesion probability maps and binary masks, yielding estimates of total lesion count and lesion volume.

Each BOLD run underwent skull-stripping, head motion and slice-timing correction, and co-registration to the T1-weighted image. Confound regressors were estimated, non-steady-state volumes were removed, and Independent Component Analysis Automatic Removal of Motion Artifacts was applied. The data were smoothed with a 6 mm FWHM Gaussian kernel, normalized to Montreal Neurological Institute space and projected to surface space. First- and second-level general linear model analyses were conducted in SPM12. For each participant, behavioral and timing files were generated from the social navigation task using a custom Python script. Behavioral files included interaction type, character identity, event onsets, reaction times, and parametric modulators (cosine of the vector angle and vector length). Timing files specified the onsets, durations, and types of task events. Two separate first-level general linear models were modeled per participant: both included regressors for narrative and decision trials, and were additionally modulated by either vector angle cosine or vector length. The six motion parameters were included as nuisance regressors in both models. All regressors and their temporal derivatives were convolved with the canonical hemodynamic response function and contrasted against baseline. Second-level (group-level) analyses included both ROI and whole-brain approaches. ROI analyses tested for BOLD signal modulation by vector angle cosine in the hippocampus and by vector length in the PPCC, based on prior literature²⁹. Whole-brain exploratory analyses were also conducted. All functional analyses, including those conducted within the predefined ROI, were performed on a voxel-wise basis. One-sample t-tests were used to assess within-group effects, and two-sample unpaired t-tests were used to assess between-group differences. Statistical maps were thresholded at a voxel-wise level of $p < 0.001$ (uncorrected), with cluster-level correction for multiple comparisons using FWE at $p < 0.05$.

Diffusion tensor imaging data were processed with the FMRIB Software Library Diffusion Toolbox⁷⁹. Geometric distortions were corrected using reversed-phase-encoding images, followed by eddy-current and head motion correction with gradient reorientation. Nonbrain tissue was removed, and the diffusion tensor model was fitted within a subject-specific white matter mask to generate fractional anisotropy and mean diffusivity maps. A lesion mask from 3D T2-FLAIR was co-registered to diffusion space and subtracted from the white matter mask, which was further refined by removing voxels with fractional anisotropy ≤ 0.2 . Mean fractional anisotropy and mean diffusivity were then extracted from the resulting normal-appearing white matter mask.

Statistical analyses

Normality of continuous behavioral, clinical, and demographic variables was assessed using the Shapiro–Wilk test, except for vector angle cosine and vector length metrics, which were analyzed using parametric two-way ANOVA. As detailed in Supplementary Table S1, the variables age, total HADS score, MacArthur–Employment, total number of relapses, EDSS score, and most importantly, number of correct answers in episodic social memory recall questionnaire did not follow a normal distribution. Therefore, nonparametric tests were consistently used, with the exception of cosine and length of social vectors.

Between-group comparisons for continuous variables were conducted using the Mann–Whitney U test, and categorical variables were analyzed using Fisher’s exact test. Associations between continuous variables were evaluated with Spearman’s rank correlation coefficient. For social navigation metrics (cosine of vector angle and vector length), we conducted two-way ANOVAs with group (MS vs. healthy controls) as a between-subject factor and character identity (C1–C5) as a within-subject factor, followed by Tukey’s post-hoc tests.

To control for potential confounders - specifically, age, sex, education level, and total HADS score - we used linear regression models to predict episodic memory recall scores. The residuals from these models, representing variance unexplained by those covariates, were then compared between groups using the Mann–Whitney U test and used in correlation analyses.

Descriptive statistics for each variable were selected to reflect the nature of the distribution and are specified in the figure legends. Statistical significance was defined as $p < 0.05$ (two-tailed).

All Mann–Whitney U tests were performed in IBM SPSS Statistics version 29.0, and other statistical tests and data visualizations were conducted in Prism version 10 (GraphPad Software).

Data availability

The datasets generated and analyzed during the current study are available from the corresponding author upon reasonable request.

Received: 16 June 2025; Accepted: 3 October 2025

Published online: 10 November 2025

References

- Jakimovski, D. et al. Multiple sclerosis. *Lancet* **403**, 183–202 (2024).
- Rocca, M. A. et al. Current and future role of MRI in the diagnosis and prognosis of multiple sclerosis. *Lancet Reg. Heal - Eur* **44**, 100978 (2024).
- DeLuca, G. C., Yates, R. L., Beale, H. & Morrow, S. A. Cognitive impairment in multiple sclerosis: Clinical, radiologic and pathologic insights. in *Brain Pathology* (ed. International Society of Neuropathology) vol. 25 79–98 (Blackwell Publishing Ltd, (2015).
- Hakim, E. A. et al. The social impact of multiple sclerosis - A study of 305 patients and their relatives. *Disabil. Rehabil.* **22**, 288–293 (2000).
- Morrow, S. A. et al. Predicting loss of employment over three years in multiple sclerosis: clinically meaningful cognitive decline. *Clin. Neuropsychol.* **24**, 1131–1145 (2010).
- Devonshire, V. et al. The global adherence project (GAP): A multicenter observational study on adherence to disease-modifying therapies in patients with relapsing–remitting multiple sclerosis. *Eur. J. Neurol.* **18**, 69–77 (2011).
- Ruet, A. et al. Cognitive impairment, health-related quality of life and vocational status at early stages of multiple sclerosis: A 7-year longitudinal study. *J. Neurol.* **260**, 776–784 (2013).
- Campbell, J., Rashid, W., Cercignani, M. & Langdon, D. Cognitive impairment among patients with multiple sclerosis: associations with employment and quality of life. *Postgrad. Med. J.* **93**, 143–147 (2017).
- Benedict, R. H. B., Amato, M. P., DeLuca, J. & Geurts, J. J. G. Cognitive impairment in multiple sclerosis: clinical management, MRI, and therapeutic avenues. *Lancet Neurol.* **19**, 860–871 (2020).
- Adolphs, R. The neurobiology of social cognition. *Curr. Opin. Neurobiol.* **11**, 231–239 (2001).
- Roheger, M., Grothe, L., Hasselberg, L., Grothe, M. & Meinzer, M. A systematic review and meta-analysis of socio-cognitive impairments in multiple sclerosis. *Sci Rep* **14**, 7096 (2024).
- Mike, A. et al. Disconnection mechanism and regional cortical atrophy contribute to impaired processing of facial expressions and theory of mind in multiple sclerosis: A structural MRI study. *PLoS One* **8**, e82422 (2013).
- Batista, S. et al. Impairment of social cognition in multiple sclerosis: amygdala atrophy is the main predictor. *Mult. Scler. J.* **23**, 1358–1366 (2017).
- Czekóová, K. et al. Impaired self-other distinction and subcortical gray-matter alterations characterize socio-cognitive disturbances in multiple sclerosis. *Front Neurol* **10**, 525 (2019).
- Labbe, T. P. et al. Regional brain atrophy is related to social cognition impairment in multiple sclerosis. *Arq. Neuropsiquiatr.* **79**, 666–676 (2021).
- Yokote, H., Okano, K. & Toru, S. Theory of Mind and its neuroanatomical correlates in people with multiple sclerosis. *Mult Scler. Relat. Disord* **55**, 103156 (2021).
- Batista, S. et al. Theory of Mind and executive functions are dissociated in multiple sclerosis. *Arch. Clin. Neuropsychol.* **33**, 541–551 (2018).
- Batista, S. et al. Disconnection as a mechanism for social cognition impairment in multiple sclerosis. *Neurology* **89**, 38–45 (2017).
- Adamaszek, M., Krüger, S., Kessler, C., Hosten, N. & Hamm, A. Clinical and neurophysiological patterns of impairments to emotion attention and empathy in multiple sclerosis. *J Integr. Neurosci* **21**, 7 (2022).

20. Isernia, S. et al. Theory of Mind network in multiple sclerosis: A double Disconnection mechanism. *Soc. Neurosci.* **15**, 544–557 (2020).
21. Koubyr, I. et al. Amygdala network reorganization mediates the theory of Mind performances in multiple sclerosis. *J. Neurosci. Res.* **100**, 537–550 (2022).
22. Labbe, T. P. et al. Social cognition in multiple sclerosis is associated to changes in brain connectivity: A resting-state fMRI study. *Mult Scler. Relat. Disord* **45**, 102333 (2020).
23. Golde, S. et al. Distinct functional connectivity signatures of impaired social cognition in multiple sclerosis. *Front Neurol* **11**, 507 (2020).
24. Biseco, A. et al. Resting-State functional correlates of social cognition in multiple sclerosis: an explorative study. *Front Behav. Neurosci* **13**, 276 (2020).
25. Okuyama, T. Social memory engram in the hippocampus. *Neurosci. Res.* **129**, 17–23 (2018).
26. Oliva, A. Neuronal ensemble dynamics in social memory. *Curr Opin. Neurobiol* **78**, 102654 (2023).
27. Cum, M. et al. A systematic review and meta-analysis of how social memory is studied. *Sci Rep* **14**, 2221 (2024).
28. Deen, B., Schwiedrzik, C. M., Sliwa, J. & Freiwald, W. A. Specialized networks for social cognition in the primate brain. *Annu. Rev. Neurosci.* **46**, 381–401 (2023).
29. Tavares, R. M. et al. A map for social navigation in the human brain. *Neuron* **87**, 231–243 (2015).
30. Zhang, L. et al. A specific brain network for a social map in the human brain. *Sci Rep* **12**, 1773 (2022).
31. Meira, T. et al. A hippocampal circuit linking dorsal CA2 to ventral CA1 critical for social memory dynamics. *Nat Commun* **9**, 4163 (2018).
32. Brissart, H., Morel, E., Baumann, C. & Debouverie, M. Verbal episodic memory in 426 multiple sclerosis patients: impairment in encoding, retrieval or both? *Neurol. Sci.* **33**, 1117–1123 (2012).
33. Borne, A., Lemaitre, C., Bulteau, C., Baci, M. & Perrone-Bertolotti, M. Unveiling the cognitive network organization through cognitive performance. *Sci Rep* **14**, 11645 (2024).
34. Scotte, N. L. et al. Regional hippocampal atrophy in multiple sclerosis. *Brain* **131**, 1134–1141 (2008).
35. Wagner, A. D., Shannon, B. J., Kahn, I. & Buckner, R. L. Parietal lobe contributions to episodic memory retrieval. *Trends Cogn. Sci.* **9**, 445–453 (2005).
36. Flanagan, V. L. et al. The precuneus as a central node in declarative memory retrieval. *Cereb. Cortex.* **33**, 5981–5990 (2023).
37. Ciampi, E. et al. Relationship between social cognition and traditional cognitive impairment in progressive multiple sclerosis and possible implicated neuroanatomical regions. *Mult Scler. Relat. Disord.* **20**, 122–128 (2018).
38. Chalah, M. A. et al. Theory of Mind in multiple sclerosis: A neuropsychological and MRI study. *Neurosci. Lett.* **658**, 108–113 (2017).
39. Koenig, K. A. et al. Hippocampal volume is related to cognitive decline and fornix diffusion measures in multiple sclerosis. *Magn. Reson. Imaging.* **32**, 354–358 (2014).
40. Chard, D. T. et al. Brain atrophy in clinically early relapsing-remitting multiple sclerosis. *Brain* **125**, 327–337 (2002).
41. Ge, Y. et al. Brain atrophy in relapsing-remitting multiple sclerosis: fractional volumetric analysis of Gray matter and white matter. *Radiology* **220**, 606–610 (2001).
42. Calabrese, M. et al. Cortical atrophy is relevant in multiple sclerosis at clinical onset. *J. Neurol.* **254**, 1212–1220 (2007).
43. Roosendaal, S. D. et al. Grey matter volume in a large cohort of MS patients: relation to MRI parameters and disability. *Mult Scler. J.* **17**, 1098–1106 (2011).
44. Magliozzi, R. et al. A gradient of neuronal loss and meningeal inflammation in multiple sclerosis. *Ann. Neurol.* **68**, 477–493 (2010).
45. Wegner, C., Esiri, M. M., Chance, S. A., Palace, J. & Matthews, P. M. Neocortical neuronal, synaptic, and glial loss in multiple sclerosis. *Neurology* **67**, 960–967 (2006).
46. Horakova, D., Kalincik, T., Blahova, D., Dusankova, J. & Dolezal, O. Clinical correlates of grey matter pathology in multiple sclerosis. *BMC Neurol* **12**, 10 (2012).
47. Geurts, J. J. G., Calabrese, M., Fisher, E. & Rudick, R. A. Measurement and clinical effect of grey matter pathology in multiple sclerosis. *Lancet Neurol.* **11**, 1082–1092 (2012).
48. Amato, M. et al. Neocortical volume decrease in relapsing-remitting MS patients with mild cognitive impairment. *Neurology* **63**, 89–93 (2004).
49. Amato, M. et al. Association of neocortical volume changes with cognitive deterioration in relapsing-remitting multiple sclerosis. *Arch. Neurol.* **64**, 1157–1161 (2007).
50. Poppenk, J., Evensmoen, H. R., Moscovitch, M. & Nadel, L. Long-axis specialization of the human hippocampus. *Trends Cogn. Sci.* **17**, 230–240 (2013).
51. Strange, B. A., Witter, M. P., Lein, E. S. & Moser, E. I. Functional organization of the hippocampal longitudinal axis. *Nat. Rev. Neurosci.* **15**, 655–669 (2014).
52. Morais-Ribeiro, R. et al. Differential atrophy along the longitudinal hippocampal axis in Alzheimer's disease. *Eur. J. Neurosci.* **59**, 3376–3388 (2024).
53. Houtchens, M. et al. Thalamic atrophy and cognition in multiple sclerosis. *Neurology* **69**, 1213–1223 (2007).
54. Batista, S. et al. Basal ganglia, thalamus and neocortical atrophy predicting slowed cognitive processing in multiple sclerosis. *J. Neurol.* **259**, 139–146 (2012).
55. Meira, T., Coelho, A., Onat, S., Ruano, L. & Cerqueira, J. J. One-year regional brain volume changes as potential predictors of cognitive function in multiple sclerosis: a pilot study. *Ir. J. Med. Sci.* **193**, 957–965 (2024).
56. Filley, C. M. & Fields, R. D. Glial cells and neuronal signaling white matter and cognition: making the connection. *J. Neurophysiol.* **116**, 2093–2104 (2016).
57. Wang, Y. & Olson, I. R. The Original Social Network: White Matter and Social Cognition. *Trends in Cognitive Sciences* vol. 22 504–516 at (2018). <https://doi.org/10.1016/j.tics.2018.03.005>
58. Yildiz, M., Tettenborn, B., Radue, E. W., Bendfeldt, K. & Borgwardt, S. Association of cognitive impairment and lesion volumes in multiple sclerosis - A MRI study. *Clin. Neurol. Neurosurg.* **127**, 54–58 (2014).
59. Engl, C. et al. Cognitive impairment in early MS: contribution of white matter lesions, deep grey matter atrophy, and cortical atrophy. *J. Neurol.* **267**, 2307–2318 (2020).
60. Lucchinetti, C. et al. Heterogeneity of multiple sclerosis lesions: implications for the pathogenesis of demyelination. *Ann. Neurol.* **47**, 707–717 (2000).
61. Trapp, B. D. et al. Axonal transection in the lesions of multiple sclerosis. *N Engl. J. Med.* **338**, 278–285 (1998).
62. Patrikios, P. et al. Remyelination is extensive in a subset of multiple sclerosis patients. *Brain* **129**, 3165–3172 (2006).
63. Bagnato, F. et al. Imaging chronic active lesions in multiple sclerosis: a consensus statement. *Brain* **147**, 2913–2933 (2024).
64. Allen, I. V., McQuaid, S., Mirakhor, M. & Nevin, G. Pathological abnormalities in the normal-appearing white matter in multiple sclerosis. *Neurol. Sci.* **22**, 141–144 (2001).
65. Mirmosayyeb, O. et al. Association between diffusion tensor imaging measurements and cognitive performances in people with multiple sclerosis: A systematic review and meta-analysis. *Mult Scler. Relat. Disord* **94**, 106261 (2025).
66. Akbar, N. et al. Diffusion tensor imaging abnormalities in cognitively impaired multiple sclerosis patients. *Can. J. Neurol. Sci.* **37**, 608–614 (2010).
67. Okuyama, T., Kitamura, T., Roy, D. S., Itoharu, S. & Tonegawa, S. Ventral CA1 neurons store social memory. *Sci. (80-)* **353**, 1536–1541 (2016).

68. Dudek, S. M., Alexander, G. M. & Farris, S. Rediscovering area CA2: unique properties and functions. *Nat. Rev. Neurosci.* **17**, 89–102 (2016).
69. Raam, T., McAvoy, K. M., Besnard, A., Veenema, A. & Sahay, A. Hippocampal Oxytocin receptors are necessary for discrimination of social stimuli. *Nat Commun* **8**, 2001 (2017).
70. Smith, A. S., Avram, W., Cymerblit-Sabba, S. K., Song, A., Young, W. S. & J. & Targeted activation of the hippocampal CA2 area strongly enhances social memory. *Mol. Psychiatry.* **21**, 1137–1144 (2016).
71. Piskorowski, R. A. et al. Age-Dependent specific changes in area CA2 of the hippocampus and social memory deficit in a mouse model of the 22q11.2 deletion syndrome. *Neuron* **89**, 163–176 (2016).
72. Donegan, M. L. et al. Coding of social novelty in the hippocampal CA2 region and its disruption and rescue in a 22q11.2 microdeletion mouse model. *Nat. Neurosci.* **23**, 1365–1375 (2020).
73. Thompson, A. J. et al. Diagnosis of multiple sclerosis: 2017 revisions of the McDonald criteria. *The Lancet Neurology* vol. 17 162–173 at (2018). [https://doi.org/10.1016/S1474-4422\(17\)30470-2](https://doi.org/10.1016/S1474-4422(17)30470-2)
74. Li, X., Morgan, P. S., Ashburner, J., Smith, J. & Rorden, C. The first step for neuroimaging data analysis: DICOM to NIfTI conversion. *J. Neurosci. Methods.* **264**, 47–56 (2016).
75. Esteban, O. et al. fMRIPrep: a robust preprocessing pipeline for functional MRI. *Nat. Methods.* **16**, 111–116 (2019).
76. Fischl, B. *FreeSurfer Neuroimage* **62**, 774–781 (2012).
77. Schmidt, P. et al. An automated tool for detection of FLAIR-hyperintense white-matter lesions in multiple sclerosis. *Neuroimage* **59**, 3774–3783 (2012).
78. Friston, K. J. et al. Statistical parametric maps in functional imaging: A general linear approach. *Hum. Brain Mapp.* **2**, 189–210 (1994).
79. Jenkinson, M., Beckmann, C. F., Behrens, T. E. J., Woolrich, M. W. & Smith, S. M. *FSL Neuroimage* **62**, 782–790 (2012).

Acknowledgements

This work was supported by a grant from the Foundation for Science and Technology (FCT) - project EXPL/MEC-NEU/0888/2021.

Author contributions

A.M. and M.M. contributed equally to this work. A.M. adapted the social memory assessment tools to Portuguese, set up the MRI acquisition pipeline, participated in participant recruitment, conducted behavioral assessments, performed neuroimaging analyses, and contributed to drafting the initial manuscript. M.M. was involved in participant recruitment, conducted behavioral data analyses, performed clinic-radiological correlations, led figure preparation, and was the main contributor to the first manuscript draft. L.A. contributed to the development of the experimental protocol, ensuring compliance with ethical and methodological standards. A.C. provided technical support for MRI acquisition and analysis. R.M.R. assisted in participant recruitment. C.G. was responsible for MRI data acquisition. T.G.O. contributed to the experimental design and interpretation of results. M.S. supported experimental design and provided technical expertise for MRI acquisition and analysis. J.C. contributed to the experimental design and participant recruitment. T.M. conceived the original idea, led the study design, coordinated collaboration among authors and institutions, secured and managed funding, performed behavioral and imaging data analyses, and was responsible for writing the manuscript.

Declarations

Competing interests

T.G.O. has served as a consultant for Sonae and Guidepoint, received speaker fees from Eisai, and had conference fees covered by Roche and Lilly. The remaining authors declare no competing interests.

Additional information

Supplementary Information The online version contains supplementary material available at <https://doi.org/10.1038/s41598-025-23153-1>.

Correspondence and requests for materials should be addressed to T.M.

Reprints and permissions information is available at www.nature.com/reprints.

Publisher's note Springer Nature remains neutral with regard to jurisdictional claims in published maps and institutional affiliations.

Open Access This article is licensed under a Creative Commons Attribution-NonCommercial-NoDerivatives 4.0 International License, which permits any non-commercial use, sharing, distribution and reproduction in any medium or format, as long as you give appropriate credit to the original author(s) and the source, provide a link to the Creative Commons licence, and indicate if you modified the licensed material. You do not have permission under this licence to share adapted material derived from this article or parts of it. The images or other third party material in this article are included in the article's Creative Commons licence, unless indicated otherwise in a credit line to the material. If material is not included in the article's Creative Commons licence and your intended use is not permitted by statutory regulation or exceeds the permitted use, you will need to obtain permission directly from the copyright holder. To view a copy of this licence, visit <http://creativecommons.org/licenses/by-nc-nd/4.0/>.

© The Author(s) 2025